

AD-A277 302



②

NAVAL POSTGRADUATE SCHOOL
Monterey, California



DTIC
ELECTE
MAR 28 1994
S E D

THESIS

IMAGING SONOLUMINESCENCE

by

John D. Pietrzak

December, 1993

Thesis Advisor:
Co-Advisor:

X. K. Maruyama
A. A. Atchley

Approved for public release; distribution is unlimited.

94-08972



94 3 25 095

REPORT DOCUMENTATION PAGE			Form Approved OMB No. 0704
Public reporting burden for this collection of information is estimated to average 1 hour per response, including the time for reviewing instruction, searching existing data sources, gathering and maintaining the data needed, and completing and reviewing the collection of information. Send comments regarding this burden-estimate or any other aspect of this collection of information, including suggestions for reducing this burden, to Washington Headquarters Services, Directorate for Information Operations and Reports, 1215 Jefferson Davis Highway, Suite 1204, Arlington, VA 22202-4302, and to the Office of Management and Budget, Paperwork Reduction Project (0704-0188) Washington DC 20503.			
1. AGENCY USE ONLY (Leave blank)	2. REPORT DATE December 1993	3. REPORT TYPE AND DATES COVERED Master's Thesis	
4. TITLE AND SUBTITLE IMAGING SONOLUMINESCENCE		5. FUNDING NUMBERS	
6. AUTHOR(S) John D. Pietrzak			
7. PERFORMING ORGANIZATION NAME(S) AND ADDRESS(ES) Naval Postgraduate School Monterey CA 93943-5000		8. PERFORMING ORGANIZATION REPORT NUMBER	
9. SPONSORING/MONITORING AGENCY NAME(S) AND ADDRESS(ES)		10. SPONSORING/MONITORING AGENCY REPORT NUMBER	
11. SUPPLEMENTARY NOTES The views expressed in this thesis are those of the author and do not reflect the official policy or position of the Department of Defense or the U.S. Government.			
12a. DISTRIBUTION/AVAILABILITY STATEMENT Approved for public release; distribution is unlimited.		12b. DISTRIBUTION CODE A	
13. ABSTRACT (maximum 200 words) A bubble in a water/glycerine mixture trapped at the pressure anti-node of a resonant sound field emits broadband flashes of light. Optical magnification and imaging of the light source has given insight into the spatial extent of the sonoluminescence (SL) source. This experiment shows that the SL source has a radius less than 1.5 microns.			
14. SUBJECT TERMS Sonoluminescence,			15. NUMBER OF PAGES 36
			16. PRICE CODE
17. SECURITY CLASSIFICATION OF REPORT Unclassified	18. SECURITY CLASSIFICATION OF THIS PAGE Unclassified	19. SECURITY CLASSIFICATION OF ABSTRACT Unclassified	20. LIMITATION OF ABSTRACT UL

NSN 7540-01-280-5500

Standard Form 298 (Rev. 2-89)

Prescribed by ANSI Std. Z39-18

Approved for public release: distribution is unlimited.

IMAGING SONOLUMINESCENCE

by

John D. Pietrzak

Lieutenant, United States Navy

B. S., Virginia Polytechnic Institute and State University, 1984

Submitted in partial fulfillment of the
requirements for the degree of

MASTER OF SCIENCE IN PHYSICS

from the

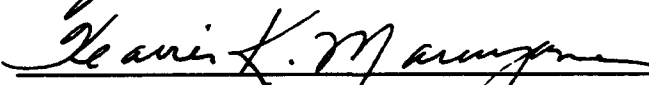
NAVAL POSTGRADUATE SCHOOL

December 1993

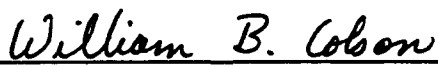
Author:


John D. Pietrzak

Approved by:


Xavier K. Maruyama, Thesis Advisor


Anthony A. Atchley, Co-Advisor


William B. Colson, Chairman,
Department of Physics

ABSTRACT

A bubble in a water/glycerine mixture trapped at the anti-node of a resonant sound field emits broadband flashes of light. Optical magnification and imaging of the light source has given insight into the spatial extent of the sonoluminescence (SL) source. This experiment shows that the SL source has a radius less than $1.5 \mu m$.

Accession For	
NTIS	CRA&I <input checked="" type="checkbox"/>
DTIC	TAB <input type="checkbox"/>
Unannounced	<input type="checkbox"/>
Justification	
By	
Distribution /	
Availability Codes	
Dist	Avail and/or Special
A-1	

Table of Contents

I. INTRODUCTION	1
A. HISTORY	1
B. THESIS OBJECTIVE	1
II. EXPERIMENTAL ARRANGEMENT AND PROCEDURE	2
A. BACKGROUND	2
B. RESONANT FLASK AND SOUND FIELD GENERATION	2
C. MAGNIFICATION AND IMAGING OF THE SL	4
D. RESOLUTION	4
E. SL PROCEDURE	5
F. TIMING	10
III. RESULTS AND DISCUSSION	13
A. INTRODUCTION	13
B. MONITOR	13
C. VARIABLE MAGNIFICATIONS	14
D. BACKLIT LASER SEQUENCE	20
IV. SUMMARY AND CONCLUSIONS	26
LIST OF REFERENCES	27
INITIAL DISTRIBUTION LIST	28

ACKNOWLEDGEMENT

The author is grateful for the assistance and professional expertise provided by the Naval Postgraduate School and the Lawrence Livermore National Laboratory. In particular, I would like to thank my thesis advisors Professor X.K. Maruyama and Professor A.A. Atchley. Their knowledge, guidance, and connections with the scientific community was invaluable.

My research was performed at Lawrence Livermore National Laboratory. I'd like to thank Dr. Michael J. Moran for his guidance throughout the experiment, Daren R. Sweider for his expertise in the experimental setup, Philip M. Armitis for the use of the Electro Optics Calibration Facility, and John E. Flatley and Thomas R. Crabtree for ideas improving the experiment.

Most of all, I am thankful for the support of my wife Pamela throughout this experience.

DISCLAIMER

The specific experimental equipment described in this work in no way constitutes an endorsement of these products.

I. INTRODUCTION

A. HISTORY

Sonoluminescence (SL) is the phenomenon of emission of visible light from microscopic gas bubbles in a liquid medium undergoing acoustic excitation. This emission of light has been known for nearly 50 years [Ref. 1]. Felipe Gaitan discovered SL emission from a single stable bubble, acoustically levitated at the pressure antinode of an acoustic standing wave setup in a laboratory flask filled with water or a water/glycerine mixture [Ref. 2]. SL is emitted once each acoustic cycle. The duration of the emission is at most tens of picoseconds. The frequency of the sound field used has a period of approximately 25 μ s. To generate SL is rather simple, to explain it is difficult. Without knowledge of the characteristics of the SL and the bubble (i.e., radius, dynamics, and spectrum), the mechanisms and theories to describe the SL phenomena will remain a mystery.

B. THESIS OBJECTIVES

The objective of this work is to optically magnify and photograph the SL phenomenon. In doing this, the size of the light source at the time of luminescence may be determined. This work was performed in collaboration with Lawrence Livermore National Laboratory (LLNL).

II. EXPERIMENTAL ARRANGEMENT AND PROCEDURE

A. BACKGROUND

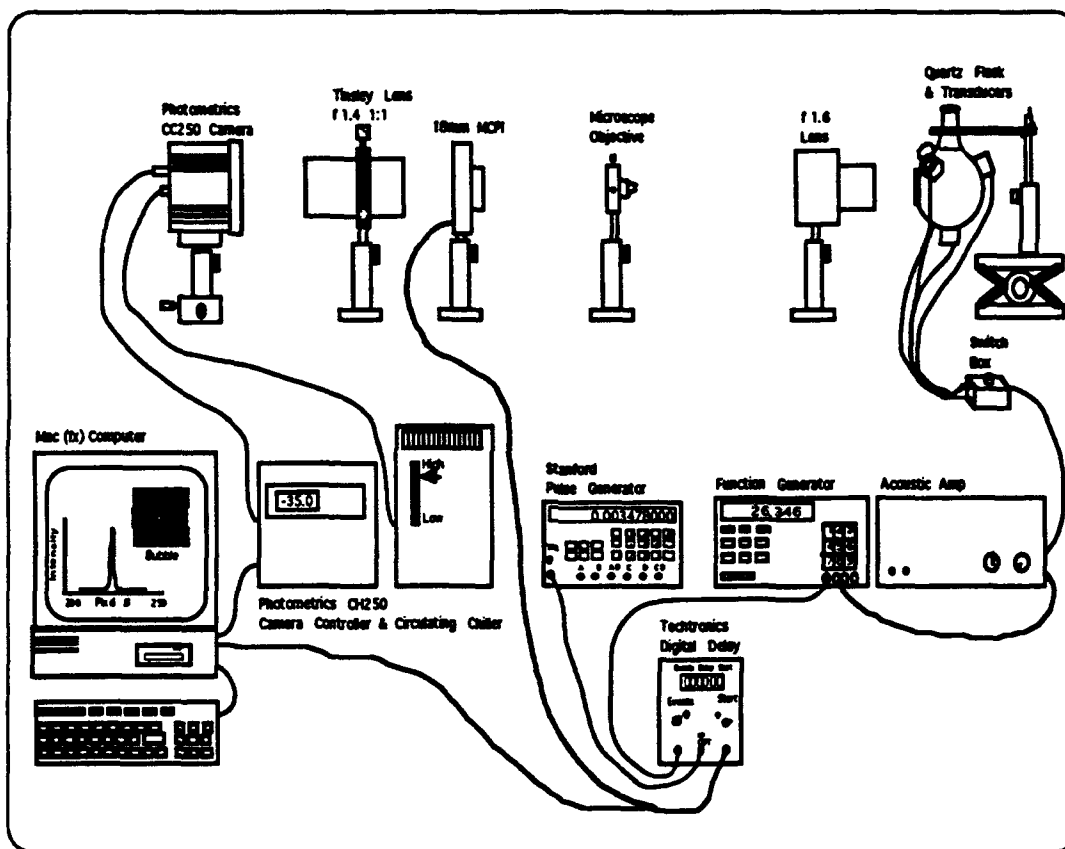
Imaging sonoluminescence (SL) required the capture of a single event, a single flash of light. The equipment must both image in low light conditions and also magnify. Figure 1 (not to scale) shows the experimental arrangement of the SL imaging system [Ref. 3]. The details of the experimental arrangement and procedure are provided in this chapter.

B. RESONANT FLASK AND SOUND FIELD GENERATION

Figure 1 outlines the experimental arrangement. The flask is a 250 ml laboratory boiling flask fitted with a 1.5 inch diameter optical quality quartz window disc. Four cylindrical piezoelectric transducers were attached in an inverted pyramid arrangement with apex on the bottom of the flask. These transducers were connected to a switch box with variable solid state resistors in series. This box is used to balance the drive signals to the individual transducers. The switch box was connected to a Techtron 5530 Audio Amplifier. The input signal was produced by a HP 8904A Function Generator.

Putterman and others have shown that the SL exhibits a much greater intensity when the water/glycerine mixture was cooled [Ref. 4]. Therefore, the flask was enclosed in a cardboard box with forced cooling air to keep the water/glycerine solution at approximately 10°C. The flask was supported on an optical table stand which could move longitudinally and transversely for focusing.

Sonoluminescence Imaging System



Sonoluminescence - Imaging Camera Experimental Setup

Figure 1 Sonoluminescence Imaging System

C. MAGNIFICATION AND IMAGING OF THE SL

The purpose of the optical lenses were to magnify the SL bubble onto a 18 mm diameter Micro-Channel Plate Intensifier (MCPI). To ensure optical clarity and to maximize the amount of light reaching the MCPI, the lenses were secured on an optical alignment track in front of the flask arrangement. All of the imaging equipment was placed on an optical table. A Cinelux-Xenon f1.6 3:1 lens was placed such that the bubble was at its focus. A microscope objective was placed at the opposite focus. The MCPI was secured on a stand after the objective stand. A Tinsley f1.4 1:1 lens was placed directly after the MCPI and in front of the Photometrics CC250 Charge-Coupled Device (CCD) camera. A HeNe laser (not shown) was used to illuminate the SL bubble to facilitate the focusing of its image into the microscope objective.

Two types of imaging were used. One was the use of a CCD camera. Its output was displayed on a video monitor. The SL was directed to the CCD camera via a mirror placed in the optical path prior to the MCPI after the microscope objective (not shown in Figure 1). This arrangement allowed for the "big picture" viewing of the SL bubble alignment onto the MCPI, bubble dynamics, and the relative intensity of SL light. The second imaging technique (detailed in Figure 1) was via the MCPI to a Photometrics CCD array CC250 camera. The Nu 200 Photometrics program in conjunction with a Macintosh FX computer was used for image processing and recording [Ref. 5]. To coordinate the timing of the SL image, a Techtronix TM5003 events delay counter and a Stanford Research Pulse Delay Generator was used for triggering the MCPI and the Photometrics camera.

D. RESOLUTION

To correctly scale the pixel size of the image produced by the MCPI/Photometrics Nu200 program and the Macintosh computer, the system resolution had to be obtained. Prior to imaging the SL, the optical setup and computer generated image had to be calibrated. This was accomplished by placing a glass

slide with etched 100 μm increments inside the flask filled with the water/glycerin solution. The flask was then backlit with white light. An image was taken with three different microscope objectives 5x, 10x, and 20x. The computer generated image magnification for the above microscope objectives was the following: 5x, 4 μm per pixel; 10x, 2 μm per pixel; and 20x, 1 μm per pixel. These images are shown in Figures 2, 3, and 4. Figure 2 shows the scale magnified with the 5x objective. There are 25 pixels between the etched lines, thus the computer image is scaled to 4 μm per pixel. Figures 3 and 4 are scaled in the same manner but with increased magnification.

Next, background images were taken to examine the performance of the MCPI. Images of no light were recorded and line out plots, relative intensity versus position plots, were produced. Figure 5 shows four different representative background plots. It shows the background intensity to be uniformly distributed. This uniform grey background is due to the accumulation of thermal counts in the CCD array. The four representative line out plots were taken from a strip of 20 images.

E. SL PROCEDURE

A solution of 20% glycerin and 80% distilled water by volume was used throughout the experiment. After the solution was shaken and stirred in a flask, it was degassed and then poured into the flask and degassed again. The solution was cooled to approximately 13°C. The solution temperature was measured with a Fluke thermocouple thermometer probe.

The function generator was turned on with the driving frequency in the range of 38 to 40 kHz and at an amplitude of 10V peak to peak. The power amplifier was also turned on and placed at an intermediate setting. With the signal switch boxes' four variable resistors (shown in Figure 1) at minimum resistance a miniature 1/8 inch diameter hydrophone was inserted into the flask to locate the resonance frequency [Ref. 6]. The resistors in the signal switch box allowed for individual adjustment of

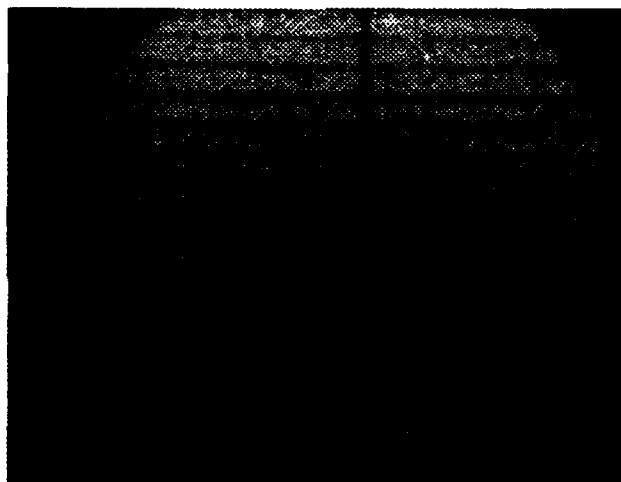


**Figure 2 5x Image of 100um Scale 25 Pixels/Division,
The Corresponding Scale Calibration is 4um/Pixel.**

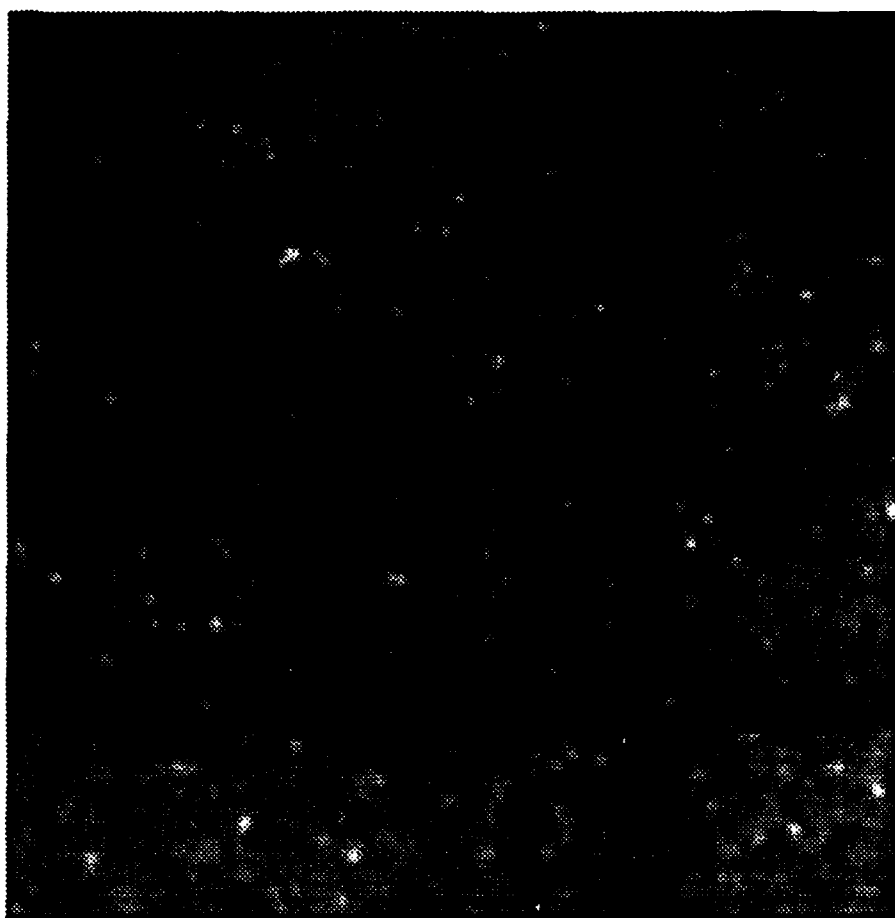
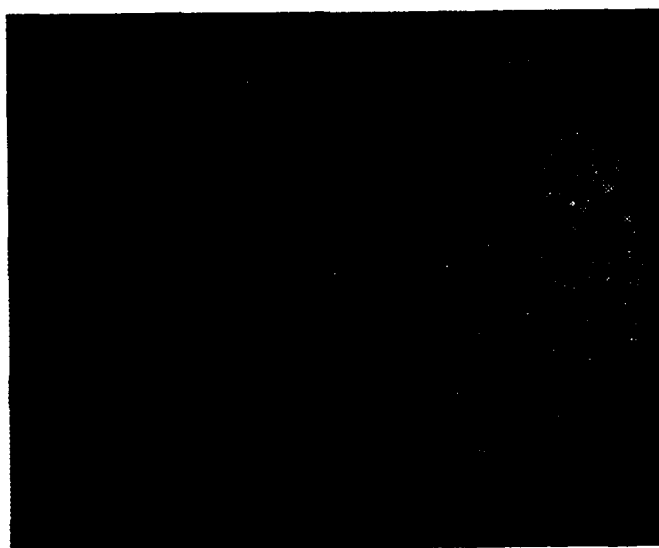


Figure 3 10x Image of 100um Scale 50 Pixels/Division,
The Corresponding Scale Calibration is 2um/Pixel.



**Figure 4 20x Image of 100um Scale 100 Pixels/Division,
Corresponding Scale Calibration is 1um/Pixel.**

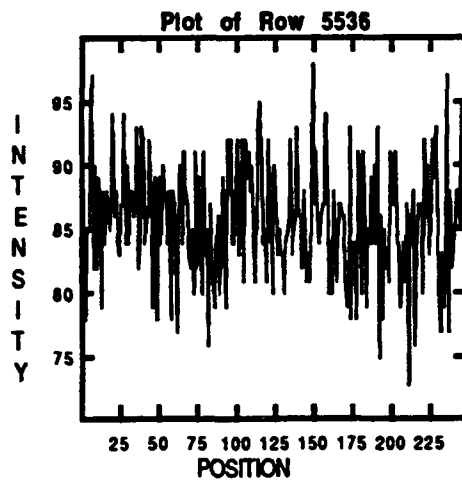
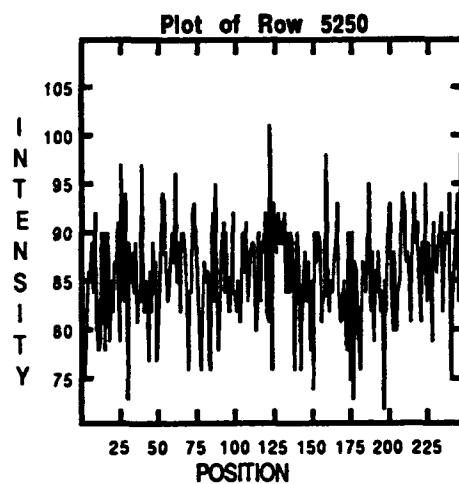
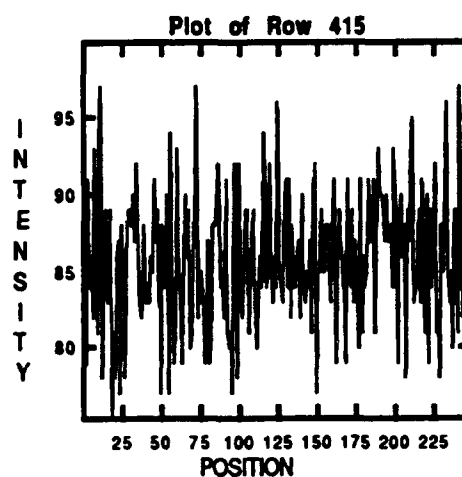
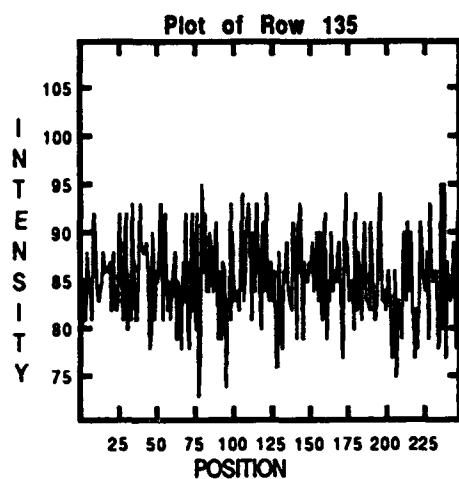


Figure 5 Four Different Line Out Plots of 20x, 1um/Pixel, of No Light Background.

the piezoelectric transducers to compensate for asymmetries induced by the flask. When a maximum hydrophone response was indicated on the oscilloscope, the frequency was recorded. At this frequency the flask was resonating with sufficient force producing high amplitude spherically symmetric standing waves in the liquid. To help locate the SL bubble, the flask was lit with low level white light and the room lights were turned off. Using a hypodermic needle, air was injected into the liquid. By simultaneously adjusting the amplitude of the power amplifier a single bubble could be captured at the pressure anti-node. When sufficient amplitude was applied, the bubble produced SL pulses. Once SL was evident the intensity was increased by adjusting either the frequency in small amounts (tens of Hertz), the amplitude, or the switch box settings to the individual transducers. Also in a similar manner, the position of the bubble could be adjusted to compensate for asymmetries induced by the flask that would cause the bubble to be displaced from the focus of the first lens.

Once a fairly stable bubble was obtained the laser was turned on to illuminate the SL bubble to aid in aligning the image of the bubble through the microscope objective. The transducers were adjusted to center the SL bubble. The micrometers on the optical stand were also used to move the image of the SL. When the alignment through the lenses was completed, the image of the SL was viewed on the television monitor via a mirror placed directly in front of the MCPI. The laser was then turned off and the SL image was adjusted to the center of the TV monitor. The driving frequency, amplitude, and switch box settings were then increased or decreased again to obtain the brightest SL.

F. TIMING

After fine focusing, the viewing mirror was removed to place the image of the SL on the MCPI. With the Nu 200 program in the focusing mode, the SL bubble was again focused with respect to the Photometrics CCD camera. The CCD camera recorded images from the MCPI. Figure 6 depicts the system timing [Ref. 7]. The

CCD camera image exposure time was set at 0.2 s for all images taken. The SL single event period was approximately 25 μ s for the frequencies used in the experiment. This signal came from the function generator and sent to the input of the Tectronics digital delay (TDD). The MCPI trigger pulse was based on the images of prior SL in the focusing mode of the Nu 200 program. The vertical dashed line (a) in Figure 6 represents when the Nu 200 program is commanded to image and turns on the CCD camera. The trigger pulse is also sent to the TDD. The Stanford Research pulse delay generator (SR) sends a delay signal and MCPI gate (on time) to the TDD. The TDD waits the required delay time and then triggers the MCPI. This is represented by the vertical dashed line (b) in Figure 6. Through an iterative process of adjusting the digital delay out and the MCPI gate on the SR within the SL period, it was possible to vary MCPI gate time. Thus varying the exposure times on the recorded SL images. Lengthening or shortening the MCPI gate as seen in Figure 6 varied exposure times from 100 μ s to 1 μ s on the MCPI. The MCPI gating time controlled the number of SL pulses that would contribute to a given image. The gating minimized spurious scintillation from the MCPI while using maximum MCPI gain. After the focusing, the camera program was switched to single or multiple strip images. These images were then saved in the Macintosh FX computer.

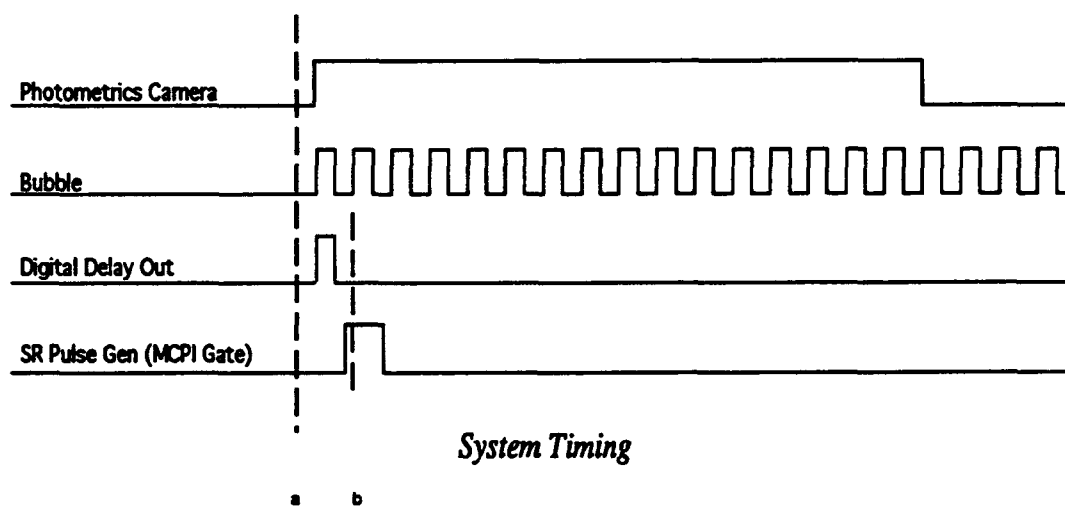


Figure 6 Sonoluminescence Imaging System Timing

III. RESULTS AND DISCUSSION

A. INTRODUCTION

The imaging system recorded images with the 5x, 10x, and 20x microscope objectives. The images were chosen for being in focus and an overall higher relative intensity. This chapter discusses the results of the experiment. The figures show recorded images and line out plots. A line out plot is a row plot of the relative intensity versus pixel position of a specific image from a single image. From these plots, the radius of the SL source may be determined by taking full width half maximum (FWHM) of the image. The intensities on the line out plots of the single events are relative to the sequence recorded. An absolute intensity calibration of the imaging system was not conducted since the experiment was directed at characterizing the radius of the SL source.

B. MONITOR

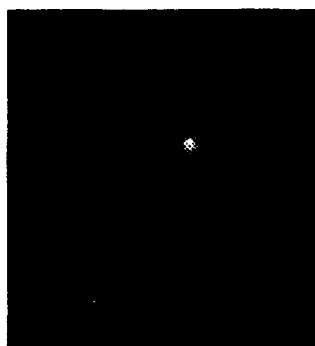
Viewing SL via the TV monitor and viewing mirror gave the capability to microscopically observe the dynamics and intensity of the SL bubble in real time. Whereas the SL bubble would look stable and bright to the naked eye, the monitor would reveal that the SL bubble was not as intense or stable as possible. The motions exhibited by the SL bubble ranged from lateral to orbital gyrations, with frequencies from a few to tens of Hertz, and the orbital radii varied from microns to millimeters. These motions did impede the ease of taking images of the SL bubble.

C. VARIABLE MAGNIFICATIONS

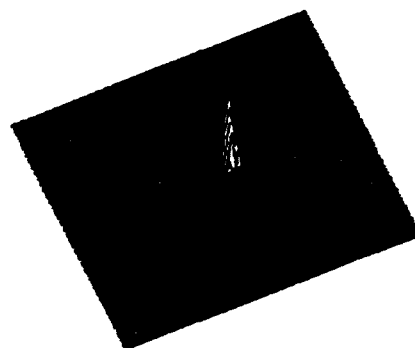
The MCPI/Photometrics imaging system recorded the SL images with three different magnifications, obtained with three microscope objectives. The images recorded showed a circular area of approximately 40 to 50 μm diameter of scattered low intensity light and a intense smaller core. The scattered region was a relatively circular area for long exposures of the order of hundreds of microseconds. When the exposure time of the MCPI was gated to less than 20 μs this diffuse region was asymmetric and less intense.

Figure 7 is SL imaged through the 5x microscope objective. The exposure time of the MCPI was 100 μs (containing four SL pulses). A larger scattered light region is quite visible and there is a bright core. The surface plot shows that there is a single source. The higher intensity core region displayed good stability, remaining in approximately the same position for long periods of time. The line out plot shows that the SL source at FWHM is about 4 pixels or 16 μm in diameter. To further investigate the SL source the exposure time of the MCPI was reduced to a single event. The surface plots of the varying MCPI exposure times are shown in Figure 8. A single source can be seen in the two single events (a and b). Figure 8c shows the results for a 320 μs exposure containing 12 pulses. From the results of Figures 7 and 8 one can conclude that SL is produced from a single source region. By selecting the peak intensity in the centroid of the SL image its size may be determined. Figure 9 is the line out plots of the surface plots from Figure 8. The size of the SL source for a single event (Figure 9a and b corresponding to Figure 8a and b) at FWHM is 3 pixels which corresponds to a 6 μm radius. For the multiple event (approximately 12 periods) shown in figure 9c, the radius of the luminescence was 8 μm . The larger radius of the multiple event may be due to SL source moving.

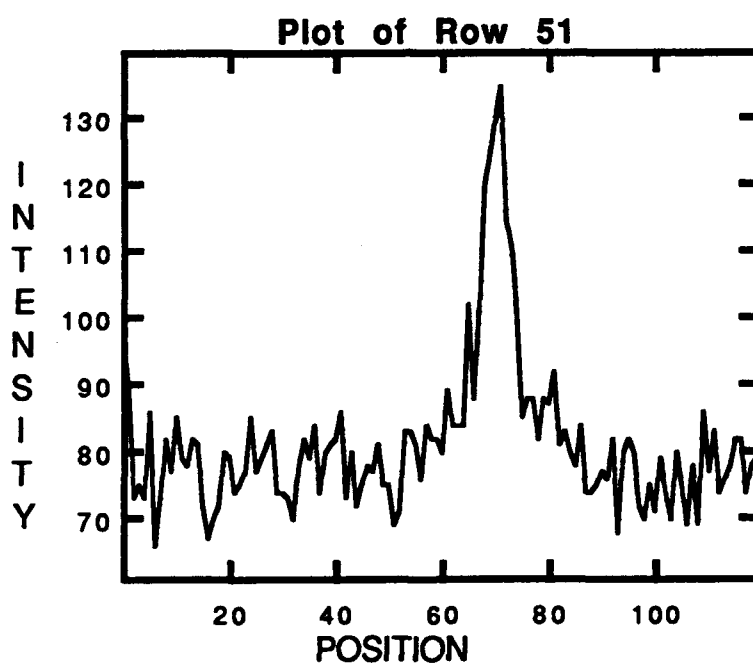
The SL source was then imaged with the 10x microscope objective. With this objective the images are scaled to 2 μm per pixel. A strip of single events were taken. The same strip of images are shown in Figures 10 and 11. In Figure 10,



(a)

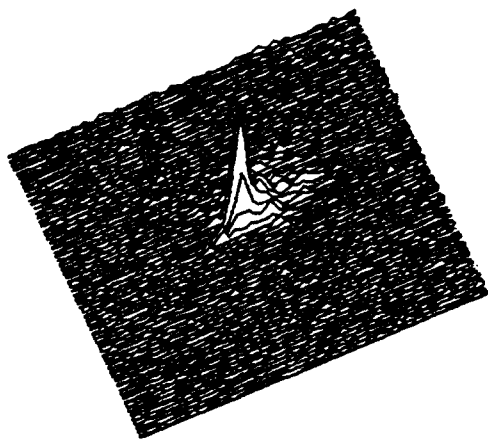


(b)

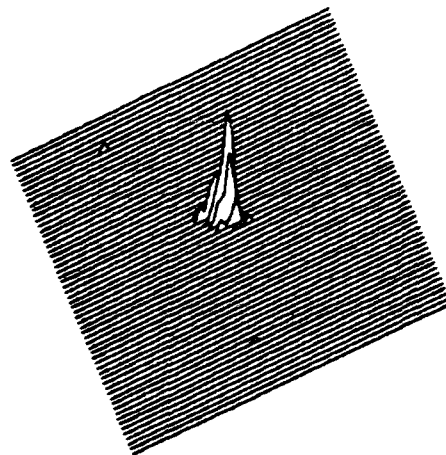


(c)

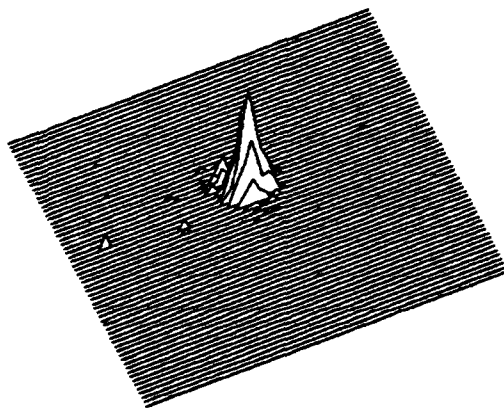
Figure 7 5x Magnification, (a) 100 us Image, (b) Surface Plot, and (c) Line Out Plot (scale of 4 $\mu\text{m}/\text{pixel}$)



(a)

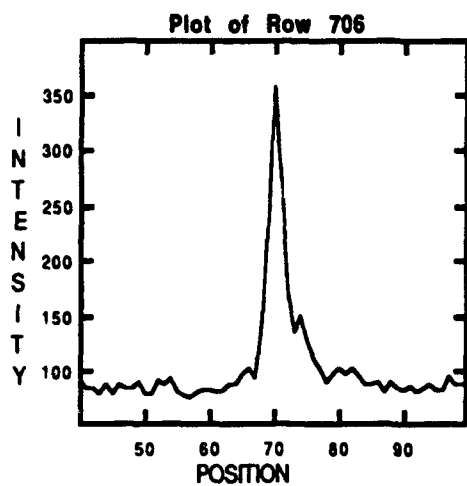


(b)

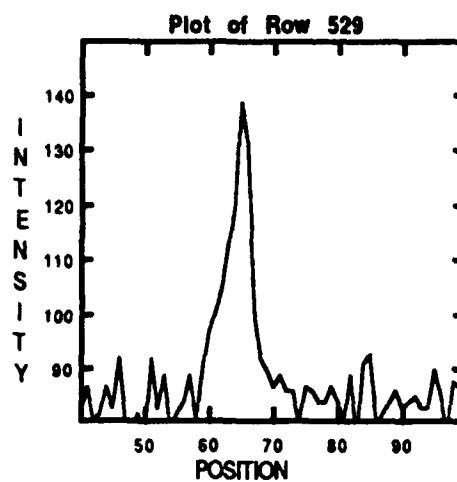


(c)

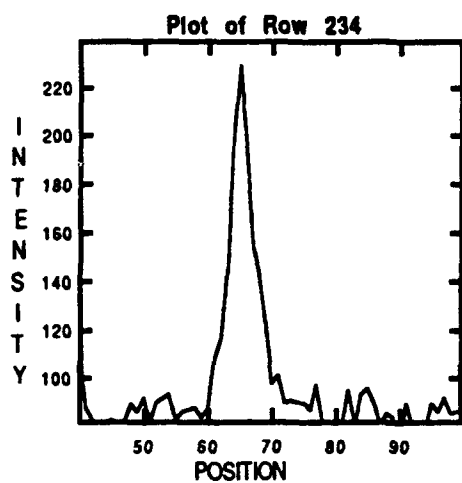
Figure 8 5x Magnification (4 $\mu\text{m}/\text{Pixel}$) Surface Plots of Varying MCPI Exposure Times, (a) 10 μs , (b) 20 μs , (c) 320 μs .



(a)



(b)



(c)

Figure 9 5x Magnification (4 $\mu\text{m}/\text{Pixel}$) Line Out Plots of Varying MCPI Exposure Time, (a) 10 μs , (b) 20 μs , and (c) 320 μs

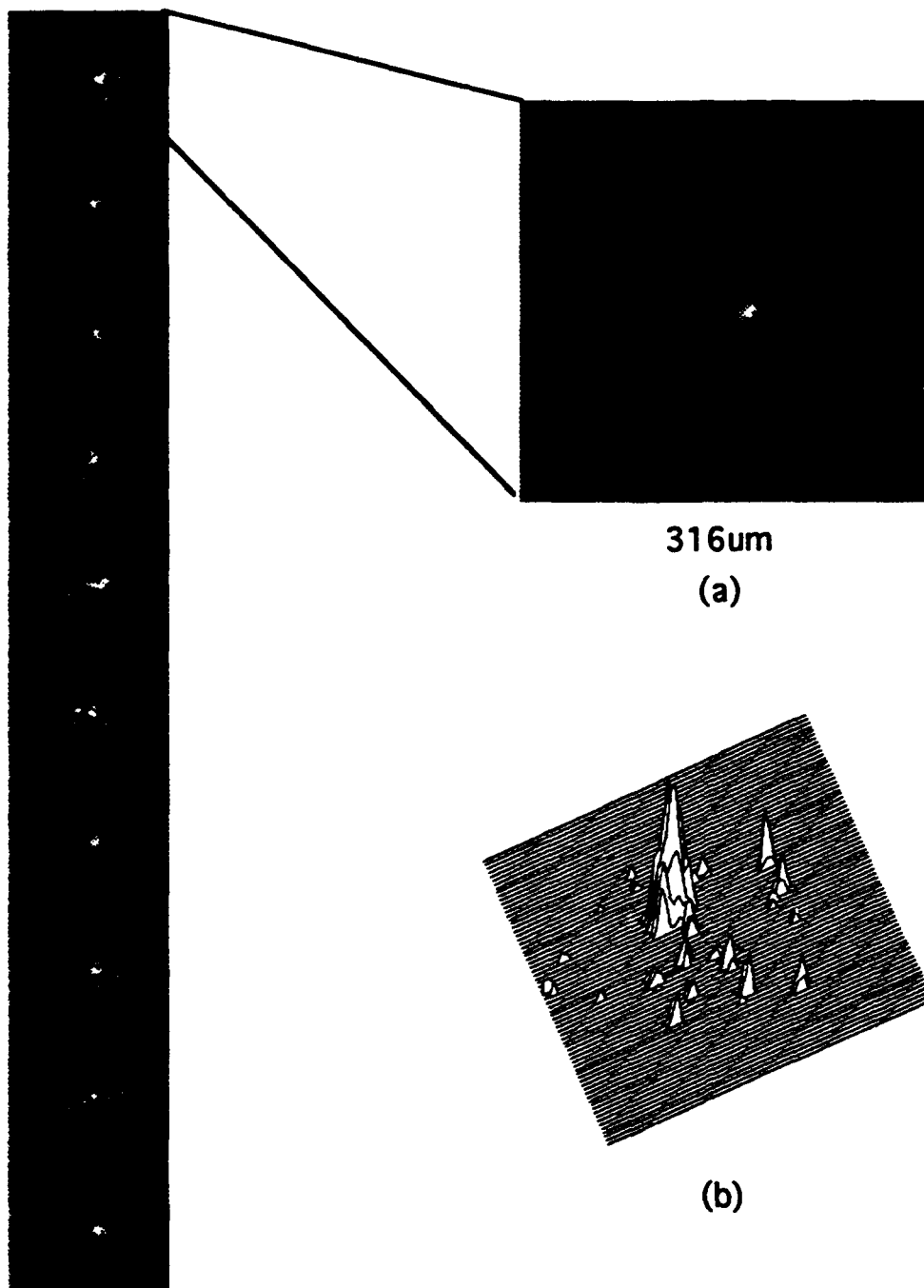


Figure 10 10x Magnification (2 $\mu\text{m}/\text{Pixel}$) Strip of 1 μs Single Event Images, (a) Frame 1, (b) and Surface Plot of Frame 1

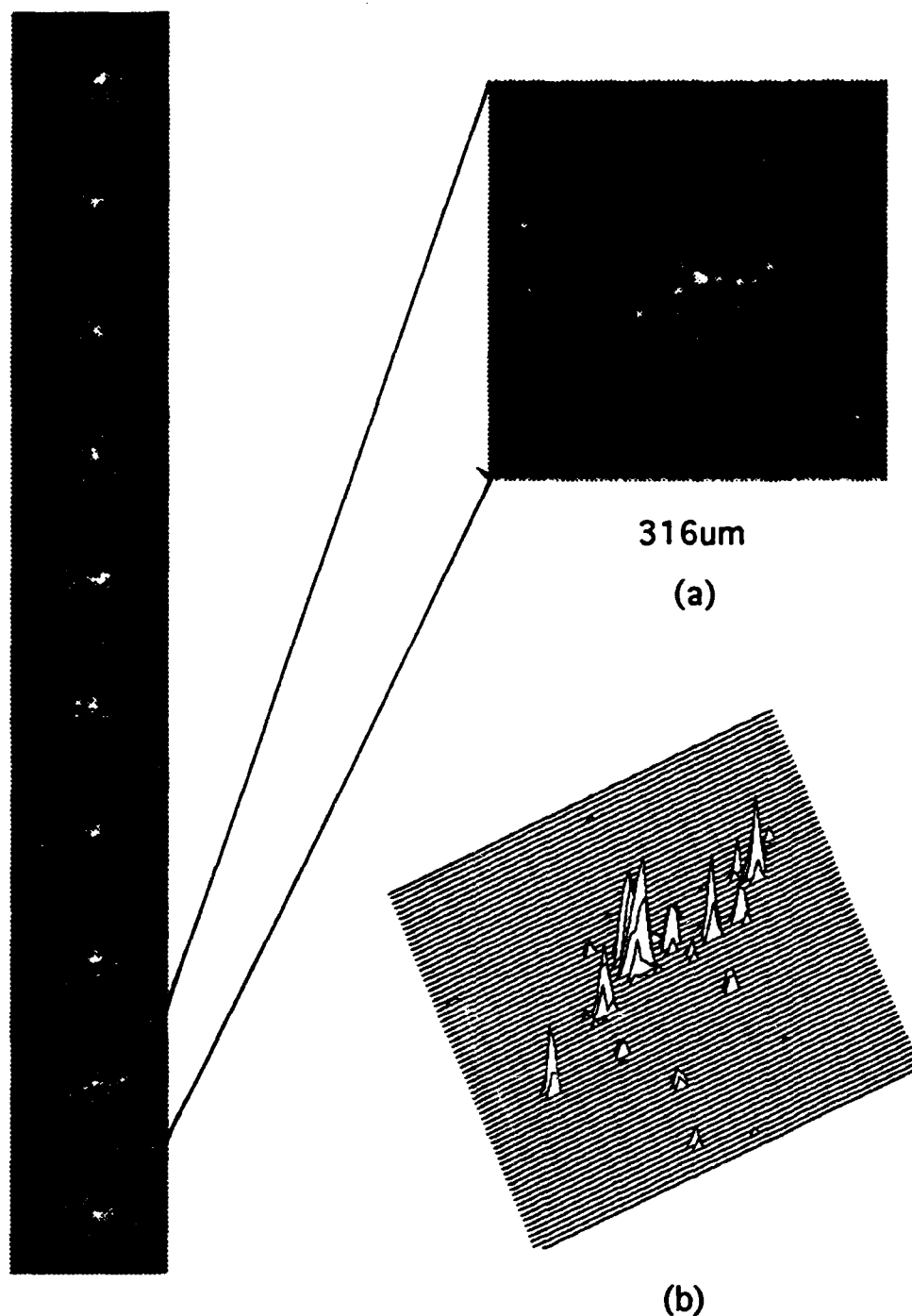


Figure 11 10x Magnification (2 $\mu\text{m}/\text{Pixel}$) Strip of 1 μs Single Event Images, (a) Frame 9, (b) and Surface Plot of Frame 9

frame 1 is enlarged to show the SL source. It can be seen that there is a bright compact center and an asymmetric diffuse region present. A surface plot is taken of the same frame, as seen in Figure 10b. This surface plot shows the core of luminescence and smaller lower intensity light surrounding it. Figure 11 is the same strip of images but with frame 9 enlarged to be investigated. The SL image does not look as compact as frame 1. However, the surface plot of frame 9 still shows a compact SL core. The surrounding peaks may possibly be due to the MCPI not having a uniform voltage potential for the $1\text{ }\mu\text{s}$ exposure time or to reflection effects from the lenses and flask window. Using the highest relative intensity peak as the centroid of the SL source, line out plots of single events were recorded. Figure 12 shows the line out plots of four different single events taken at a scaled magnification of $4\text{ }\mu\text{m}$ per pixel. At FWHM these plots show that the SL source is 3 to 4 pixels in diameter. Figure 13 is four different single events imaged with the 10x microscope objective, $2\text{ }\mu\text{m}$ per pixel. Again the FWHM diameter is 3 pixels. The same result is the case, as seen in Figure 14, when the SL source is imaged with a 20x microscope objective. The FWHM diameter is $3\text{ }\mu\text{m}$ at $1\text{ }\mu\text{m}$ per pixel. For all magnifications, the smaller brighter region was never observed to be larger than the imaging system resolution, which was 3 pixels. This result puts an upper bound on the SL source size. The SL source radius is less than $1.5\text{ }\mu\text{m}$.

D. BACKLIT LASER SEQUENCE

Another experiment was conducted to study the motion of the SL bubble. A HeNe laser was placed behind the flask at approximately 30° angle above the horizon looking down at the bubble. A sequence of images were taken with the MCPI gate at $1\text{ }\mu\text{s}$. The MCPI gate or trigger was then shifted by $1\text{ }\mu\text{s}$ through the single event period, taking 30 images. The duration of the sequence was about 60 seconds. Shifting the MCPI gate through the period of a single event simulates the taking of images in a "streak camera" like fashion. Figure 15 shows the images taken.

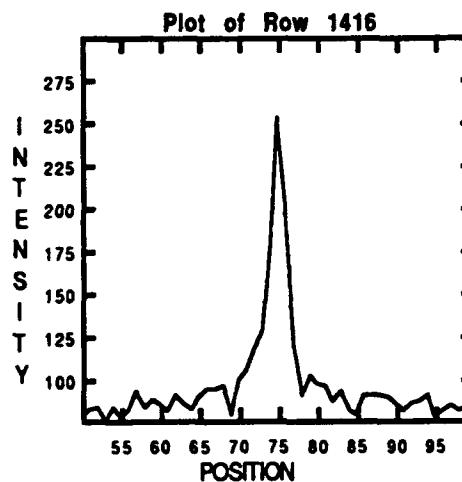
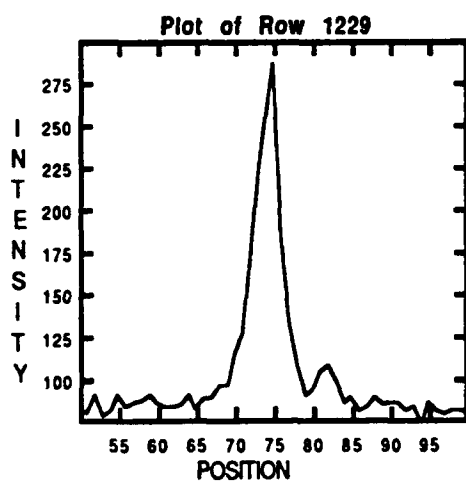
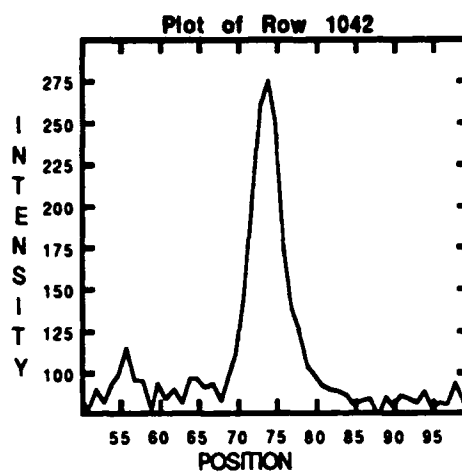
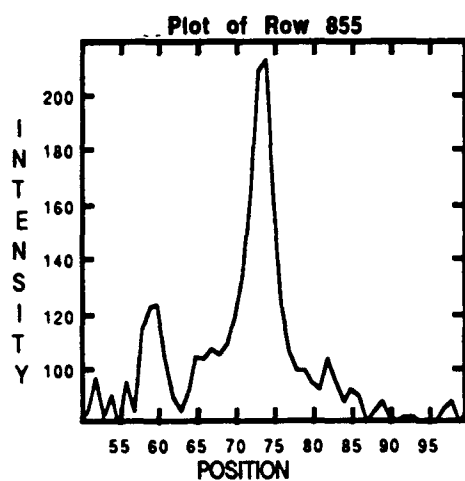


Figure 12 5x Magnification (4 $\mu\text{m}/\text{Pixel}$) Line Out Plots of Four Different 1 μs Single Events

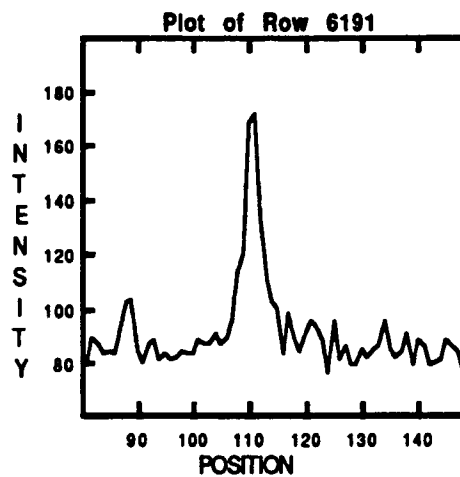
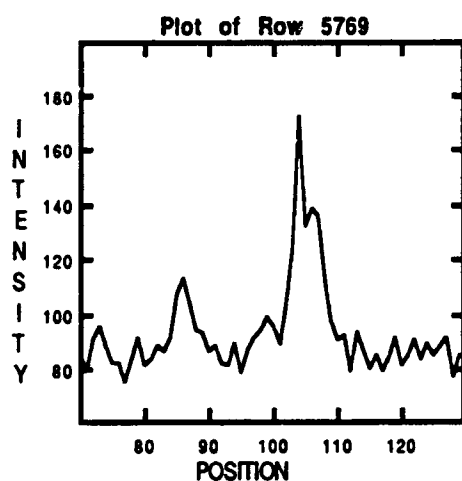
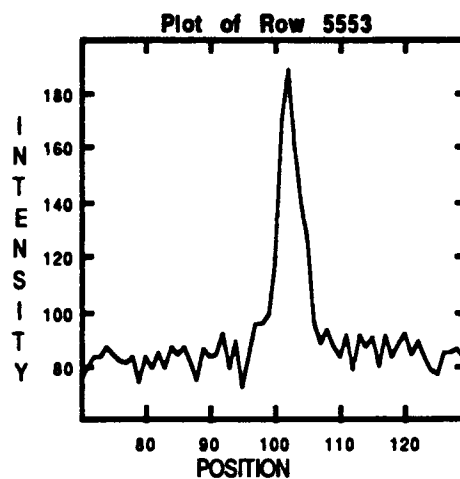
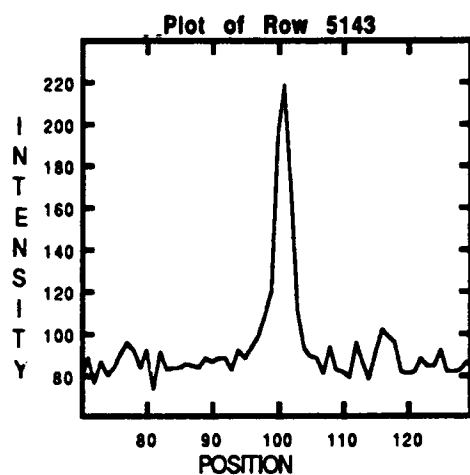


Figure 13 10x Magnification (2 $\mu\text{m}/\text{Pixel}$) Line Out Plots of Four Different 1 μs Single Events

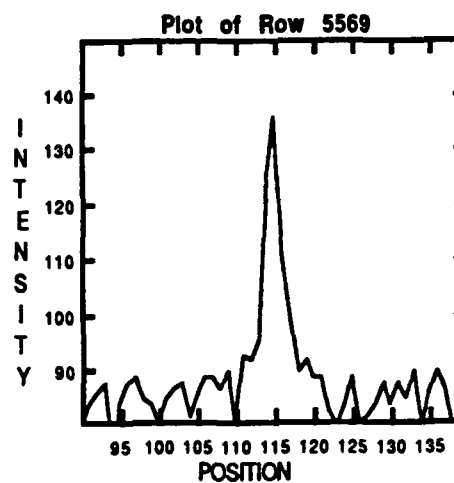
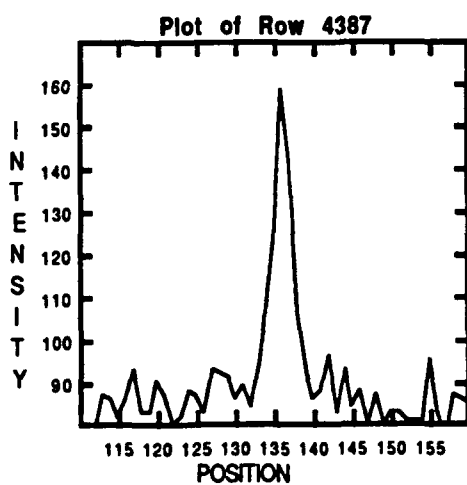
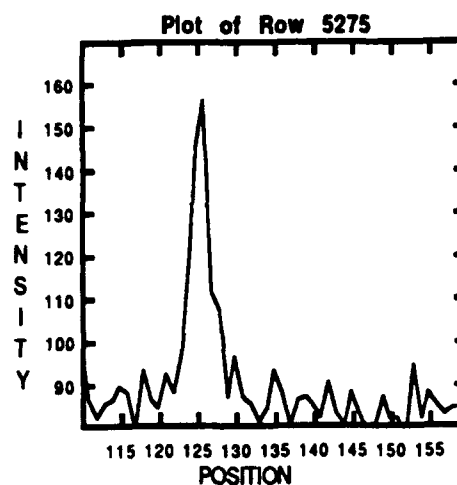
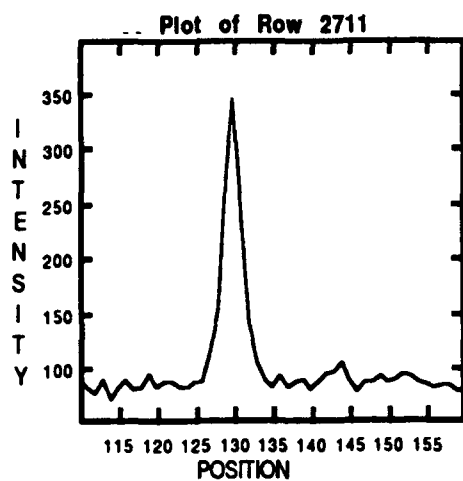


Figure 14 20x Magnification (1 $\mu\text{m}/\text{Pixel}$) Line Out Plots of Four Different 1 μs Single Events

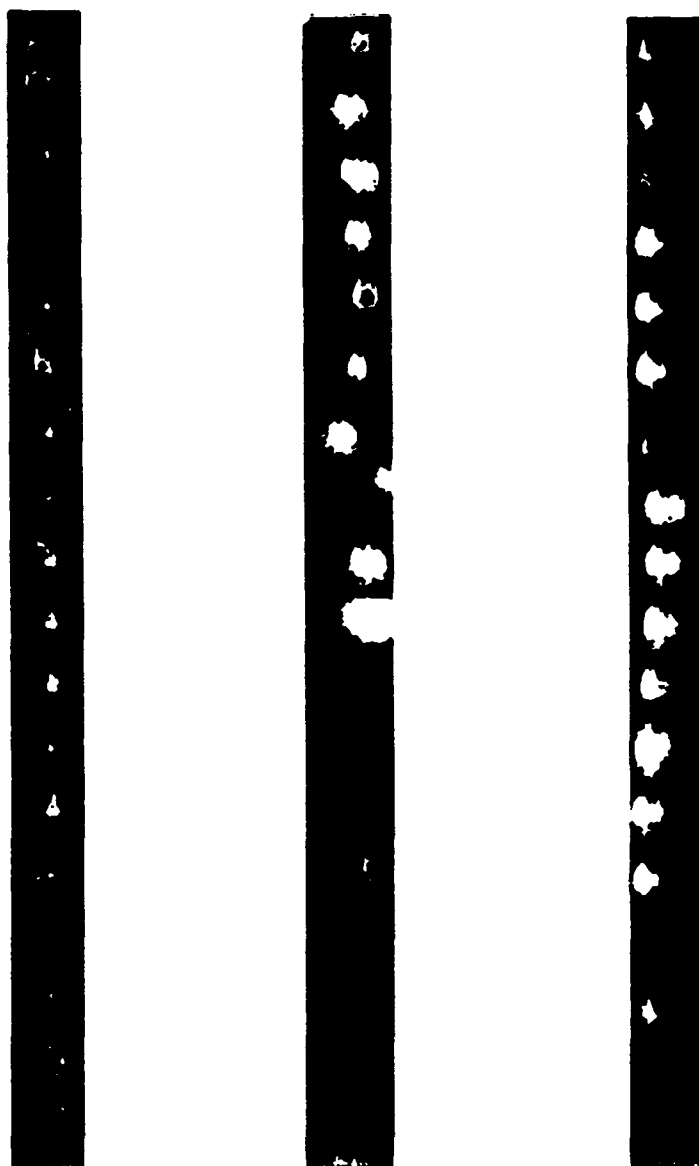


Figure 15 "Streak Like" Images of SL Taken with Varying Microscope Objectives, Left to Right 5x, 10x, and 20x

The image frames are 188 by 188 pixels. The magnifications are from left to right 5x, 10x, and 20x. It can be seen that the SL bubble motion can be as much as tens of microns. This motion may adversely affect small diameter optical fiber recording the luminescence. This motion may have been the reason that Carlson seen variations in his recorded intensities whereas Lewia did not [Ref. 8, 9]. Carlson had used a 100 μm fiber and Lewia used a 600 μm fiber.

This experiment was not intended to study Mie scattering but may revealed something about the dynamics of the bubble. In Figure 15, one can see that the scattered light from the laser increases and decreases through out the single event period. This may possibly be due to the SL bubble radius motion.

IV. SUMMARY AND CONCLUSION

This experiment places an upper bound on the size of the SL source. A Mie scattering experiment completed by Barber and Putterman resulted in a minimum SL bubble radius of $4\text{ }\mu\text{m}$ at the time of luminescence [Ref. 10]. The Mie scattering experiment conducted at NPS to determine the minimum radius at the time of luminescence resulted in a minimum SL bubble radius of approximately $3\text{ }\mu\text{m}$ [Ref. 11]. Hydrodynamic simulation performed at LLNL using the hydrocode KYNDA resulted in a minimum bubble radius of $1\text{ }\mu\text{m}$ at the time of luminescence and suggests that the SL source radius is smaller than the bubble radius, on the order of hundredths of microns [Ref. 12]. This experiment improves upon the previous experimental efforts by measuring the SL source size rather than the bubble size. The source radius is determined to be less than $1.5\text{ }\mu\text{m}$ at the time of luminescence, which is in agreement with the theoretical conclusions.

LIST OF REFERENCES

1. Frenzel and Schultes, Z. Physik. Chem. **27**, 1934.
2. Gaitan, F., Crum, L., Church, C., Roy, R., "Sonoluminescence and Bubble Dynamics for a Single, Stable, Cavitation Bubble", J. Acoust. Soc. Am., **91**, 1992.
3. Figure 1 prepared by Daren Sweider, Electro Optics Calibration Facility, Lawrence Livermore National Laboratory.
4. Hiller, R., Putterman, S. , Barber, B., "Spectrum of Synchronous Picosecond Sonoluminescence", Phys. Rev. Lett., **69**, 1992.
5. Photometrics Nu 200 Camera Controller Software, 1990-1991, Photometrics LTD.
6. Constructed by Daren Sweider, Electro Optics Calibration Facility, Lawrence Livermore National Laboratory.
7. Figure 2 prepared by Daren Sweider, Electro Optics Calibration Facility, Lawrence Livermore National Laboratory.
8. J.T. Carlson, "Visible Spectrum of Stable Sonoluminescence", MS Thesis, Naval Postgraduate School, 1992.
9. S.D. Lewia, "Spectra of Stable Sonoluminescence", MS Thesis, Naval Postgraduate school, 1992.
10. Barber, B., Putterman, S., "Light Scattering Measurements of the Repetitive Supersonic Implosion of a Sonoluminescent Bubble", Submitted to Phys. Rev. Lett., September 1992.
11. W.J. Lentz, A.A. Atchley, D.F. Gaitan, and X.K. Maruyama, "Mie Scattering from a Sonoluminescing Bubble", presented at the 13th ISNA, 1993.
12. W.C. Moss, D.B. Clarke, and J.W. White, "Hydrodynamic Simulations of Bubble Collapse and Picosecond Sonoluminescence", Lawrence Livermore National Laboratory Preprint, UCRL-JC-114748, 1993.

INITIAL DISTRIBUTION LIST

- | | | |
|----|------------------------------------------|---|
| 1. | Defense Technical Information Center | 2 |
| | Cameron Station | |
| | Alexandria, Virginia 22304-6145 | |
| 2. | Library, Code 52 | 2 |
| | Naval Postgraduate School | |
| | Monterey, California 93943-5002 | |
| 3. | Professor William B. Colson, Code PH/Cw | 1 |
| | Chairman, Department of Physics | |
| | Naval Postgraduate School | |
| | Monterey, California 93943-5000 | |
| 4. | Professor Xavier K. Maruyama, Code PH/Mx | 3 |
| | Department of Physics | |
| | Naval Postgraduate School | |
| | Monterey, California 93943-5000 | |
| 5. | Professor Anthony A. Atchley, Code PH/Ay | 1 |
| | Department of Physics | |
| | Naval Postgraduate School | |
| | Monterey, California 93943-5000 | |
| 6. | Dr. Michael J. Moran | 1 |
| | University of California | |
| | Lawrence Livermore National Laboratory | |
| | P. O. Box 808, L-41 | |
| | Livermore, California 94551 | |

- | | | |
|-----|----------------------------------------|---|
| 7. | Philip M. Armatis | 1 |
| | University of California | |
| | Lawrence Livermore National Laboratory | |
| | P. O. Box 808, L-54 | |
| | Livermore, California 94551 | |
| 8. | Daren R. Sweider | 1 |
| | University of California | |
| | Lawrence Livermore National Laboratory | |
| | P. O. Box 808, L-44 | |
| | Livermore, California 94551 | |
| 9. | W. C. Moss | 1 |
| | University of California | |
| | Lawrence Livermore National Laboratory | |
| | P. O. Box 808, L-200 | |
| | Livermore, California 94551 | |
| 10. | Dr. Felipe Gaitan, Code PH/Gn | 1 |
| | Department of Physics | |
| | Naval Postgraduate School | |
| | Monterey, California 93943-5000 | |
| 11. | John D. Pietrzak | 1 |
| | 829 Boxhill Rd. | |
| | Virginia Beach, Virginia 23464 | |